SETAC PRESS

Environmental Toxicology and Chemistry, Vol. 31, No. 1, pp. 194–201, 2012
© 2011 SETAC
Printed in the USA
DOI: 10.1002/etc.728

Nanomaterials in the Environment

INTERACTIONS OF GOLD NANOPARTICLES WITH FRESHWATER AQUATIC MACROPHYTES ARE SIZE AND SPECIES DEPENDENT

J. Brad Glenn,*†‡ Sarah A. White,†§ and Stephen J. Klaine†||
†Institute of Environmental Toxicology, Clemson University, Pendleton, South Carolina, USA
‡Interdisciplinary Graduate Program in Environmental Toxicology, Clemson University, Clemson, South Carolina, USA
§Department of Environmental Horticulture, Clemson University, Clemson, South Carolina, USA
||Department of Biological Sciences, Clemson University, Clemson, South Carolina, USA

(*Submitted* 27 *June* 2011; *Returned for Revision* 6 *October* 2011; *Accepted* 11 *October* 2011)

Abstract—The partitioning of 4- and 18-nm gold nanoparticles (AuNPs) to aquatic macrophytes was investigated in vivo with exposure suspension in well water. Three morphologically distinct aquatic macrophytes were studied. *Myriophyllum simulans* Orch. and *Egeria densa* Planch. are submerged aquatic vascular plants, whereas *Azolla caroliniana* Willd. is a free-floating aquatic fern. Because aquatic plants absorb the majority of their nutrients from the water column, it is logical to hypothesize that they may absorb nanomaterials in suspension, potentially facilitating trophic transfer. Each plant was exposed to two different-sized gold nanospheres at a nominal concentration of 250 μg/L AuNPs for 24 h. Macrophytes were harvested at six time points (1, 3, 6, 12, 18, and 24 h), dried, and then analyzed for gold concentration via inductively coupled plasma–mass spectrometry. Concentrations were normalized to whole-plant dry tissue mass. The present study shows that absorption of AuNPs through root uptake was size and species dependent. Electron microscopy revealed that 4- and 18-nm AuNPs adsorbed to the roots of each species. Root tissue was sectioned, and transmission electron microscopy indicated that 4-nm and 18-nm AuNPs were absorbed by *A. caroliniana*, whereas only 4-nm AuNPs were absorbed by *M. simulans*. *Egeria densa* did not absorb AuNPs of either size. Gold nanoparticles were confirmed in tissue by using energy-dispersive X-ray spectroscopy. Absorption of AuNPs by plants may be a function of the salinity tolerance of each species. Environ. Toxicol. Chem. 2012;31:194–201. © 2011 SETAC

Keywords—Nanoparticle Aquatic macrophyte Trophic transfer Gold Sorption

INTRODUCTION

Industry research and development have been the driving force behind producing and applying many types of engineered nanoparticles (ENPs). These ENPs are used in a wide spectrum of applications, including enhancing existing products, advancing micrometer-sized technology, and developing new medical and imaging techniques. The Woodrow Wilson Center on Emerging Nanotechnologies reports that more than 1,000 products now contain or use nanomaterials (http://www.nanotechproject.org/) according to their manufacturers.

Although many types of nanomaterials exist, metallic nanoparticles (NPs) are useful because they are easily visualized, easily modified with different surface chemistries, and easily made into a wide variety of shapes and sizes [1,2]. Metallic NPs include particles made from Au, Ag, Pt, Fe, and Cu as well as quantum dots and metal oxides such as ZnO and TiO_2 particles. Among these particles, gold nanoparticles (AuNPs) are used most opportunistically because of their ease of synthesis, stability in suspension, and unique optical properties [1,3–5]. For centuries, people have taken advantage of the optical properties of AuNPs in various applications from stained glass windows to art glass. These optical properties make AuNPs easy to visualize, because the light scattered by AuNPs is in the visible range [4–6]. These unique abilities of AuNPs make them ideal for delivery, imaging, and transport studies. Also important is the fact that AuNPs are considered relatively nontoxic. Although it is generally accepted that bulk gold is safe, nanometer-sized gold is still under scrutiny [4,7,8].

Because of the increased production of nanomaterials and compounds containing nanomaterials, concern exists about the eventual release of nanomaterials into the environment. Although natural nanomaterials are present in the environment, these NPs lack the specific size range and shapes that are characteristic of ENPs [9]. These natural particles, often referred to as fine particulate matter, also lack specific surface chemistry modifications that can enhance bioavailability, stability, and in some cases toxicity. Because ENPs may interact with the environment differently from natural particulates, understanding their fate is a vital first step in proactive research and possible future regulations. Limbach et al. [10] and Kiser et al. [11] hypothesized that engineered nanomaterials entering wastewater will partition to sewage sludge and biofilms. Sludge is often applied as a soil amendment, and, if nanomaterials are present, eventual release of these nanomaterials to the environment could result [12]. Nanomaterials may be released into the aquatic environment by rain events, leaching, runoff, or direct release of nanomaterials in treated wastewater.

Proactive research on the fate of NPs is important in understanding where other types of nanomaterial may partition or interact once exposed to a freshwater aquatic system. Aquatic plants were chosen for the present study because they comprise a major portion of aquatic primary productivity; as such, they represent the base of the aquatic food web. Several studies have examined exposure of NPs to terrestrial plants such as C

Presented at Nano 2010: International Conference on the Environmental Effects of Nanomaterials, Clemson University, August, 2010.
All Supplemental Data may be found in the online version of this article.
* To whom correspondence may be addressed (jbglenn@clemson.edu).
Published online 28 October 2011 in Wiley Online Library (wileyonlinelibrary.com).

nanomaterials translocation in rice plants [13] and Cu nanomaterial exposure to wheat and mung bean [14] and several other plants [15,16], but a paucity of information exists on aquatic plant exposure. A recent study by Ferry et al. [17] examined partitioning of gold nanorods (65 nm length × 15 nm diameter) in an estuarine mesocosm. They reported little partitioning of nanorods into the salt marsh cord grass *Spartina alterniflora*. These results should not be universally applied, because *S. alterniflora* is an emergent halophyte, is able to tolerate high-salinity concentrations, and is not always submerged. *Spartina alterniflora* is in the Poaceae family and, like other grasses, absorbs nutrients through its roots. Also, because *S. alterniflora* is an emergent species, it has a thicker, waxy cuticle on the leaf and stem surface to help reduce water loss [18]. The thick cuticle on the leaves of *S. alterniflora* acts as a barrier (Supplemental Data, Fig. S1a), and the primary absorption mechanism for nutrients is the roots, where uptake from soil and sediment occurs. All of these characteristics make it a poor representative species for freshwater aquatic plants.

Aquatic macrophyte species differ in leaf morphology and nutrient acquisition mechanisms. In *Egeria densa*, for example, the cuticle is much thinner, and the leaves are only two cell layers thick (Supplemental Data, Fig. S1b and c). Submerged aquatic plants can absorb nutrients directly from the water column through their roots, as they are often not anchored to sediment. Some species can also acquire nutrients via their shoots [19]. For example, *Ceratophyllum* spp., a rootless aquatic plant, uses shoots for nutrient uptake directly from the water column [20].

In the present study, 4- and 18-nm citrate-coated gold nanospheres were used to investigate the influence of particle size on the interactions of NPs with aquatic plants. The objective of the present study was to determine whether particle size influenced AuNP uptake among different species. Secondary objectives included visualizing where the nanomaterials were sorbed with plant tissue, quantifying tissue concentrations, and determining whether NP sorption is related to macrophyte surface area. To our knowledge, this is the first study investigating the interaction of citrate-AuNPs with freshwater aquatic plants.

MATERIALS AND METHODS

NP characterization and preparation

Four- and eighteen-nanometer AuNP spheres (obtained from Catherine Murphy, University of Illinois, Urbana—Champaign) were characterized for size and morphology via transmission electron microscopy (TEM) in both stock and exposure media before and after exposure (Clemson University Advanced Materials Research Laboratory). Zeta potential measurements (Malvern Zetasizer) of 4- and 18-nm AuNP suspensions (nominal concentration of 250 μg/L) in exposure media were taken to determine stability of AuNPs in suspension. This concentration was chosen as a working concentration so that imaging of AuNPs interacting with tissues could be preformed. This is not an environmentally relevant concentration at this time. Nanoparticle suspensions were made in filtered well water (Pall Corporation type A/E glass fiber filters). Well water (alkalinity 80 mg/L $CaCO_3$, hardness 107 mg/L $CaCO_3$, pH 7.1, total organic carbon 8.56 mg/L, salinity 0.10 ppt, conductivity 210 μs/cm^3) was chosen to limit nutrients and to restrict periphyton growth during experimental exposures. For the 4- and 18-nm AuNP suspensions, each size was suspended independently in one batch before being aliquoted to test chambers, to ensure concentration uniformity. Samples were collected to verify initial (0 h) and final (24 h) concentrations.

Test plant species

Three aquatic plants were chosen for the aqueous exposures to AuNPs. These species were chosen because of their distinct leaf morphology and location within the water column. *Azolla caroliniana* is a free-floating aquatic fern that floats atop the water column and has roots that extend downward about 3 cm, with scale-like leaves. *Myriophyllum simulans* is a submergent species with finely dissected needle-like leaves, and *Egeria densa* is a submergent species with whorls of broad leaves. Both submergent species can reside floating free in the water column or can be rooted in the sediment via adventitious roots. Aquatic macrophytes were cultured in a double-layer, polyethylene-covered greenhouse at the Clemson University Institute of Environmental Toxicology. The greenhouse was maintained at 25 ± 2°C, with a photoperiod of 14:10 h light:dark. Original specimens of *E. densa* were collected from Lake Issaqueena, South Carolina, USA. *Myriophyllum simulans* was ordered from an online pet supply store, and *A. caroliniana* was obtained from constructed wetlands in Cairo, Georgia, USA. All plants selected for this study appeared healthy and had limited or no periphyton growth. Plant cultures were not axenic. Plants were rinsed vigorously with distilled water before experimental use. Experimental exposures occurred in the greenhouse during July, 2010.

Experimental design

The experiment was a 2 × 3 × 6 factorial with two AuNP sizes, three plant species, and six harvest periods. Each aquatic macrophyte was grown separately in a 70-ml glass test tube. Each treatment had three replications ($n = 3$) with three subreplications that were combined to ensure sufficient dry mass for gold detection. Each subreplicate plant was of approximately 1.0 ± 0.2 g fresh weight. Plants were harvested at 1, 3, 6, 12, 18, and 24 h; allowed to drip dry; patted with a Kimwipe; and then dried overnight at 60°C in a drying oven. Plants were not rinsed in this experiment so that any AuNPs sorbed to the surface of the macrophyte were retained. The final dry weight (g) was recorded after 24 h of drying.

Treatment suspensions were sampled, and gold concentration remaining in the test chamber was determined. Water samples from each subreplicate were combined to form one replicate for a total $n = 3$ for each harvest period per AuNP size. Collected water samples were acidified to achieve 5% final acid concentration using full-strength aqua regia (1:3 nitric acid to hydrochloric trace-grade acids) and then allowed to sit for 24 h before analyzing for gold (see below). Test chambers were acid rinsed with 10% aqua regia to recover any gold adsorbed to the chamber wall, and the rinsates were analyzed. The concentration of Au in the rinse was minimal; therefore, the results are not included.

Gold analysis

Tissue digestion was preformed based on a modified method from Anderson et al. [21]. After drying, tissue was transferred to cooled, cleaned, preweighed, 20-ml ceramic crucibles. Crucibles were cleaned before each digestion by heating to 450°C for 4 h in a muffle furnace. Dried plant material within the crucible was dry-ashed at 530°C for 14 h to facilitate breakdown of plant cellulose and lignin components. Once cooled, plant ash was

weighed, digested with 0.652 ml full-strength aqua regia, and then diluted to 6 ml to achieve 5% acid concentration for analysis using inductively coupled plasma–mass spectrometry (Thermo Scientific X series 2). All samples were centrifuged at 3,000 *g* for 9 min after acidification, so that particulates, if present, did not interfere with analysis. Water samples were analyzed using inductively coupled plasma–mass spectrometry, without further manipulation.

Colorimetric surface area analysis

We modified the colorimetric method developed by Cattaneo and Carignan [22] to estimate aquatic macrophyte surface area. For each species, 0.150 g fresh tissue was used to determine surface area. In modifying the method, we used 0.2 g/L methylene blue dye mixed with a 50:50 liquinox:ultrapure water surfactant mix. Plants were dipped into the dye mixture, shaken 30 times, and rinsed in 200 ml ultrapure water. This procedure was repeated three separate times using the same plant section. Each time, the ultrapure water was replaced and reserved. The surfactant effectively breaks the water surface tension on the plant and facilitates a uniform coating of dye across the entire plant. The dye was measurable at an absorbance of 664 nm to quantify the amount of dye in each rinse. The absorbance value of the rinsate was compared with a standard curve of terrestrial leaves with a known surface area, measured using an LI-3100C leaf surface area meter (LI-COR).

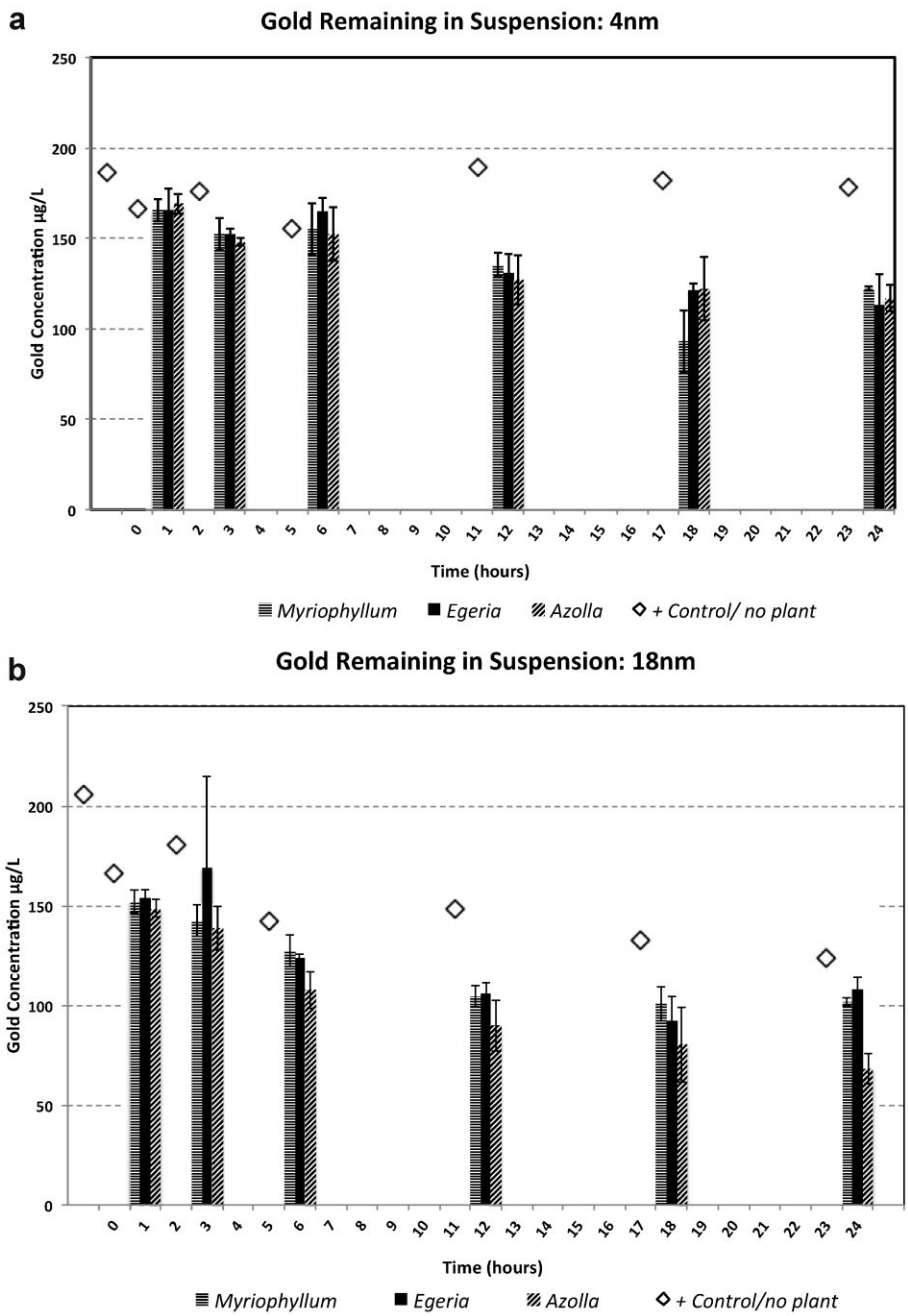

Fig. 1. Gold concentration remaining in suspension in (**a**) 4-nm and (**b**) 18-nm gold nanoparticle treatments. Error bars represent the standard deviation of the mean. Diamond represents control suspensions with no plant tissue present. First diamond is for time 0, which represents initial gold concentration. Each additional diamond shows concentration remaining in positive controls for corresponding time point. Gold concentration is significantly reduced by treatments for 12, 18, and 24 h time points. ($p < 0.05$).

Scanning electron microscopy and TEM preparation

Plant root tissue samples were prepared for TEM, scanning electron microscopy (SEM), and scanning transmission electron microscopy (STEM) by overnight fixation in 3.5% gluteraldhyde. After samples had been fixed, both TEM and SEM samples were washed in phosphate buffer at pH 7.1 three times, for 30 min each time, with a final buffer wash overnight. Samples were then washed with ultrapure water three times and dehydrated with increasing ethanol concentrations (35, 50, 70, and 95%, and then three times at 100%) for 10 min each step.

For SEM, after samples had been dehydrated, they were rinsed with a 50:50 mixture of 100% ethanol:hexamethyldisilazane, allowed to evaporate, and then rinsed with only hexamethyldisilazane and allowed to evaporate. When the samples had been dried, they were mounted onto the appropriate grid or microscopy stub.

For TEM and STEM samples, after the ethanol dehydration step, samples were embedded into a 50:50 mixture of 100% ethanol:LR White resin for 15 minutes, then embedded into 100% LR White resin, refrigerated overnight, and polymerized at 60°C in a drying oven overnight. Samples where then sectioned (90–100 nm thick) using a Leica ultramicrotome. Microscopy samples were viewed on a Hitachi HD-2000 STEM at 200 kV or on a Hitachi 4800 SE with TE detector at 25 kV (Clemson University Advanced Materials Research Laboratory). Samples were imaged on 200-mesh Si-free Cu grids. Energy dispersive X-ray spectroscopy was performed on the HD-2000 or Hitachi 4800 to confirm Au presence.

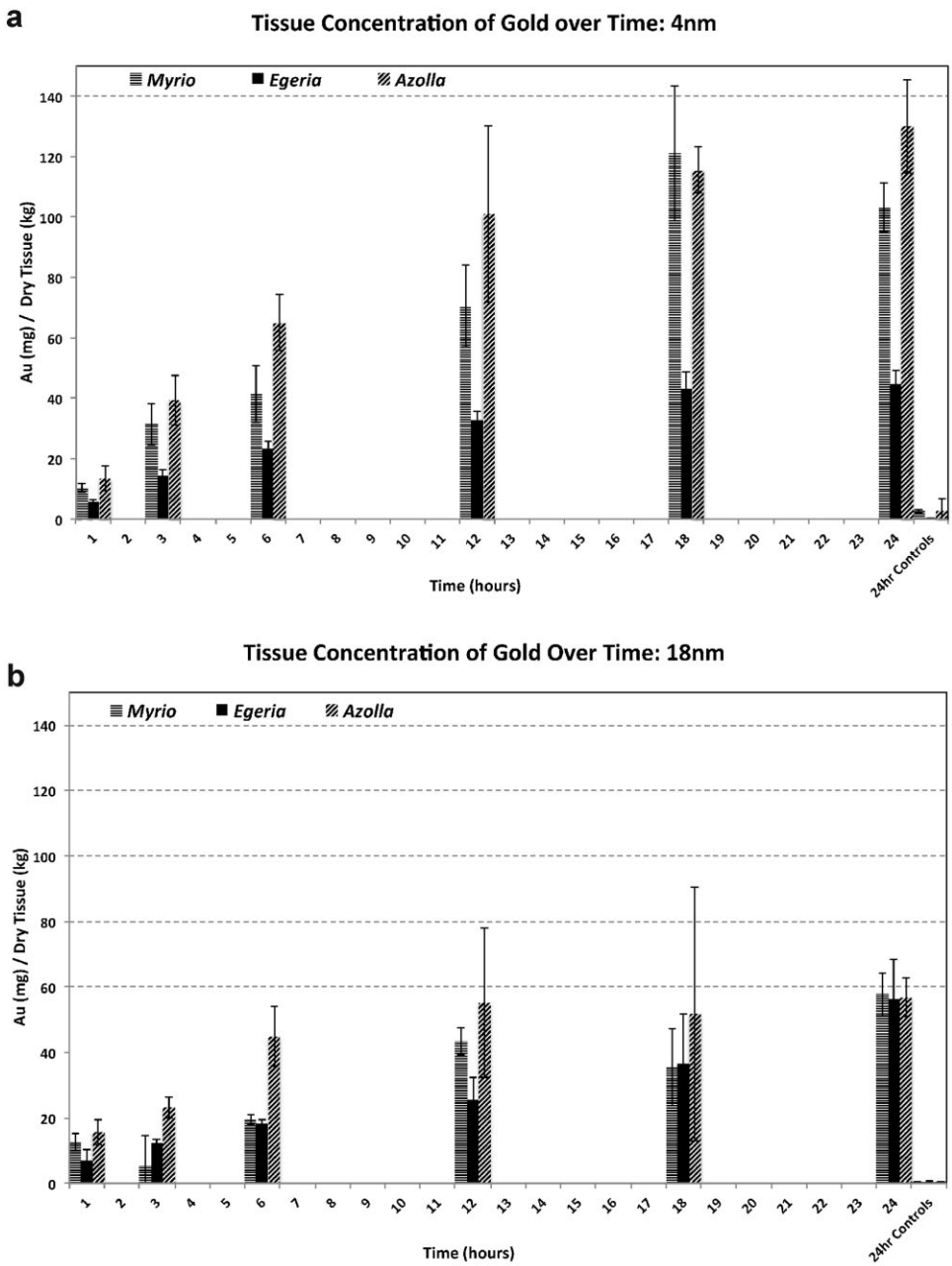

Fig. 2. Tissue concentration of gold using whole-plant. (**a**) 4-nm gold and (**b**) 18-nm gold nanoparticle treatment. Error bars represent the standard deviation of the mean. All treatments concentrations are significantly different from 24 h controls. ($p < 0.05$). 24 h controls were not exposed to gold nanoparticles.

Data analysis

Statistical analyses were performed on data in SAS (SAS Institute, Cary, NC). Slopes for sorption rate were checked for homogeneity of intercepts to determine whether slope or sorption rate had any significant differences. Analysis of variance was performed using PROC GLM to test for treatment differences. A least significant difference post hoc test was performed to quantify differences between treatments and controls ($\alpha = 0.05$).

RESULTS AND DISCUSSION

Characterization of AuNPs and treatment suspensions

Transmission electron microscopy revealed that stock AuNPs did not undergo visual changes in size or morphology during the 24-h exposure (Supplementary Data, Fig. S2). The zeta potential measurements were −14.1 mV and −9.73 mV for the 4- and 18-nm AuNPs, respectively. Positive controls, or vials containing AuNP suspensions but no plant tissue, were run for each treatment. No significant change in concentration was detected for the 4-nm AuNPs positive control treatment after 24 h compared with hour 0. Hour 0 positive control represents the initial concentration of the suspension in Figure 1a and b. However, a significant decrease in concentration occurred in the 18-nm AuNPs positive control treatment (206 μg/L to 123.5 μg/L), suggesting aggregation and settling of the 18-nm AuNPs out of the water column. Although aggregation occurred in the 18-nm AuNP treatments, a significant decrease in Au concentration was observed in the treatments with aquatic plants compared with the positive controls. After the 12-h time point, aqueous Au concentrations (Fig. 1) were reduced by approximately 38 and 32% in the 4- and 18-nm treatments containing plants, respectively, compared with positive controls.

Sorption of AuNPs with aquatic macrophytes

In the present study, we aimed to determine whether AuNPs adsorbed, absorbed, and potentially bioconcentrated within or onto aquatic macrophyte tissue. If trophic transfer of nanomaterial can occur in the environment, NP partitioning either within or on tissue surfaces is irrelevant. Tissue concentration is important, however, when determining the sorption rates and factors that influence particle sorption. In all treatments, no visual phytotoxic effects were evident. Gold accumulated in plant tissue over the 24-h exposure (Fig. 2). The data suggest that although NP sorption with *E. densa* did not differ between particle sizes, 4-nm AuNPs sorbed with *A. caroliniana* and *M. simulans* at a higher rate and in higher numbers than 18-nm particles. This difference in sorption rate and concentration may be due to differences in plant species as well as AuNP size. Plant cells have complex cell walls that support the plant and protect cells from damage and pathogens. Because nutrient uptake and cell signaling are necessary, cell walls have pores. Any particle > 40 μm or 4 nm would have difficulty passing through a pore [23]; however, it has been proposed that pore uptake could be one of multiple transport pathways [24]. Larger particles not able to pass through pores in cell walls may be able to enter through foliar structures such as stomata. Particle assimilation through stomata was reported in the terrestrial plant *Vicia faba* [24]; however, high humidity and conditions that favored stomata opening were necessary. Stomata may or may not be present in aquatic plants [25]. In the case of *A. caroliniana*, a floating vascular fern, stomata are present on the top and underside of the floating leaves [26], although plant uptake through roots seems the most plausible route, as various other studies have supported [13,16,27,28].

The presence of AuNPs in the root tissue of these aquatic macrophytes was affirmed by using electron microscopy; TEM, SEM, or STEM was used to image sections of root tissue from all species for AuNP presence. *Azolla caroliniana* images indicated that both 4- and 18-nm AuNPs were absorbed into the root, although 4-nm AuNPs were present in higher numbers (Fig. 3). Using elemental dispersive X-ray (EDX) spectroscopy, we confirmed that AuNPs were present in all images (Supplemental Data, Figs. S3 to S5). Unlike the other aquatic species studied, *A. caroliniana* roots possess root hairs that help the plant acquire nutrients. Root uptake of AuNPs by *A. caroliniana* is consistent with other reports of NP absorption by terrestrial plant roots, which also have root hairs [13,27,28]. *Myriophyllum simulans* and *E. densa* root tissue was also sectioned. In these species, 18-nm AuNPs were adsorbed on the surface of the root cells, but no uptake into cells was observed (Figs. 4a and 5a). However, *M. simulans* absorbed

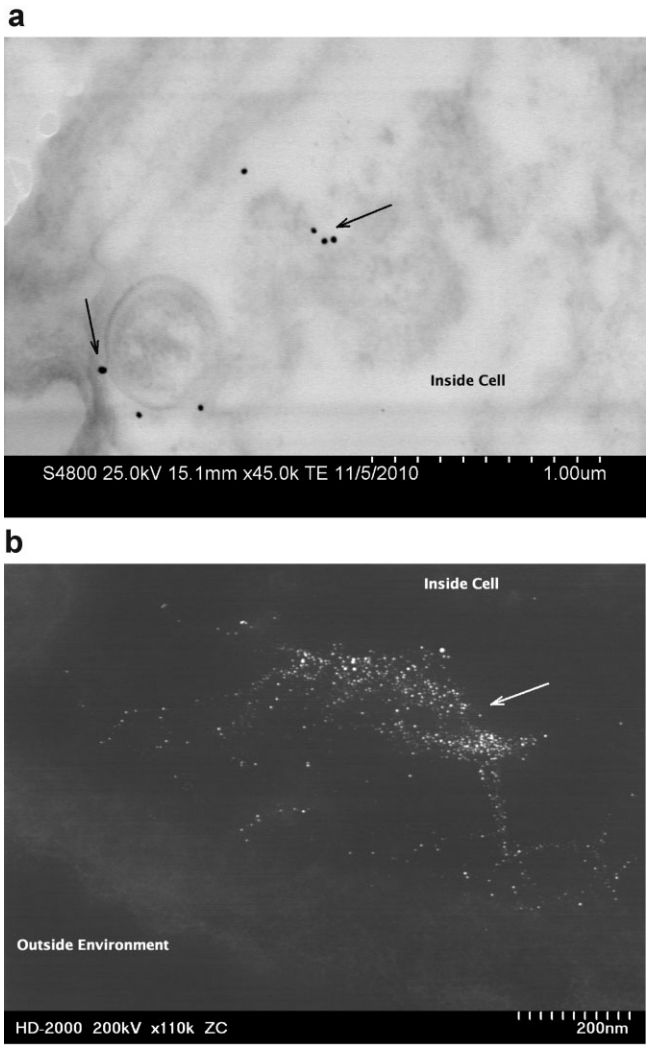

Fig. 3. Electron micrographs of *Azolla caroliniana* sectioned root tissue. Gold nanoparticles are indicated by arrows. (**a**) Transmission electron micrograph of 18-nm gold nanoparticle treatment (in which electron-dense material appears dark). (**b**) Scanning transmission electron micrograph of 4-nm gold nanoparticle treatment (in which electron-dense material appears as bright white).

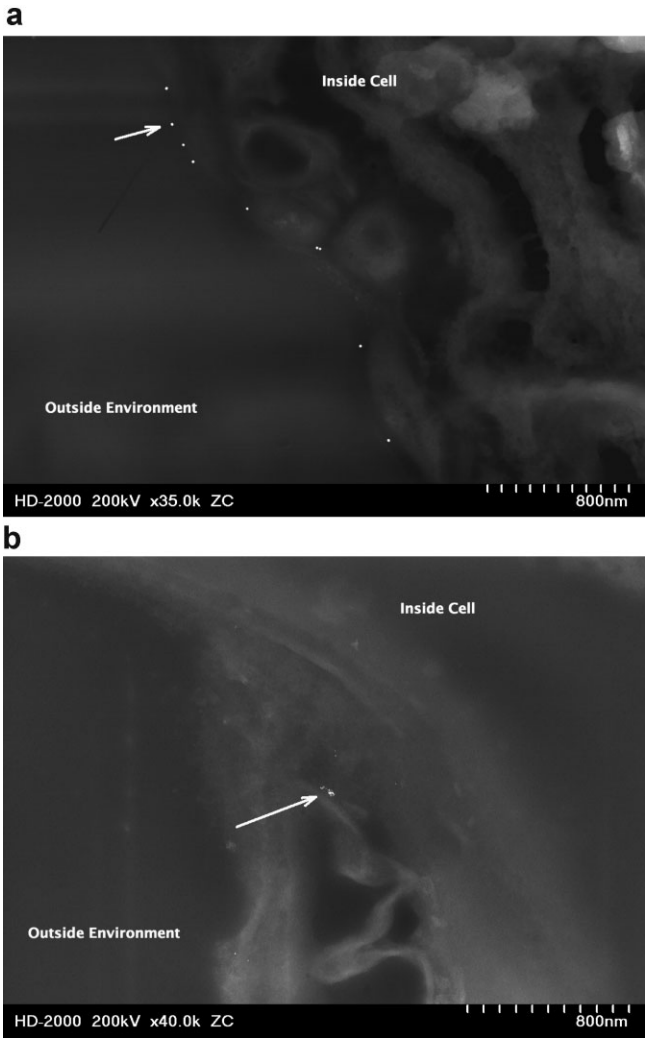

Fig. 4. Electron micrographs of *Myriophyllum simulans* sectioned root tissue. Gold nanoparticles are indicated by arrows. (**a**) Scanning transmission electron micrograph (STEM) of 18-nm gold nanoparticle treatment. (**b**) STEM micrograph of 4-nm gold nanoparticle treatment (electron-dense material appears as bright white).

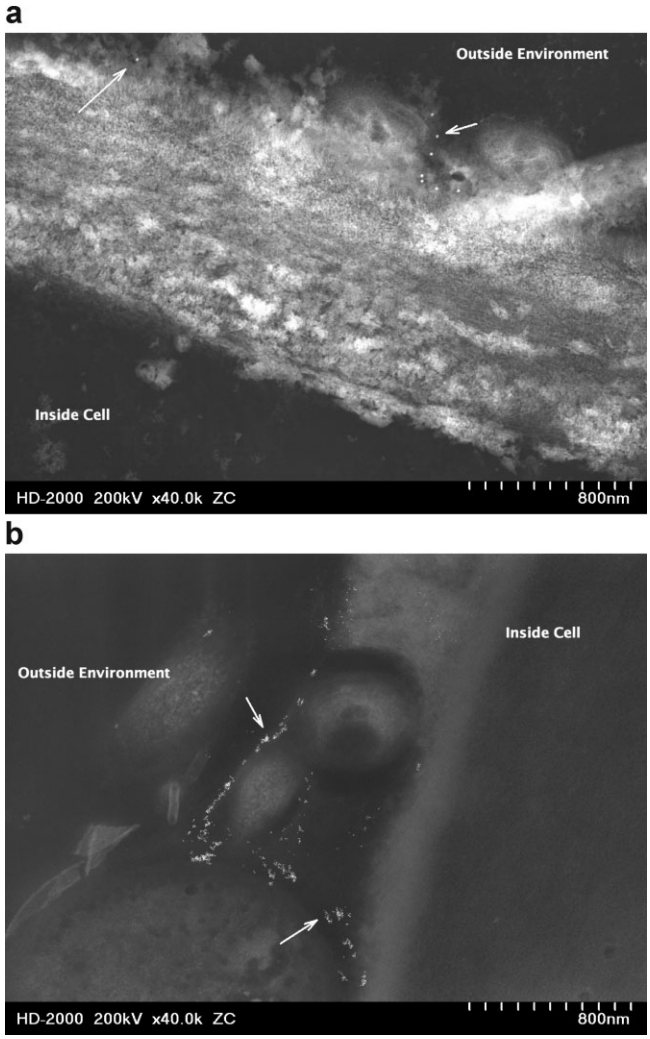

Fig. 5. Electron micrographs of *Egeria densa* sectioned root tissue. Gold nanoparticles are indicated by arrows. (**a**) Scanning transmission electron micrograph (STEM) of 18-nm gold nanoparticle treatment. (**b**) STEM micrograph of 4-nm gold nanoparticle treatment (electron-dense material appears as bright white).

4-nm AuNPs into root cells (Fig. 4b), but no uptake into *E. densa* tissue was observed (Fig. 5b). Based on these results, we conclude that AuNP uptake and partitioning are both a function of particle size and plant species.

When comparing absorption of AuNPs among these three species, a possible mechanism of AuNP exclusion could be salinity tolerance and membrane structure. Plants have developed a wide range of adaptions for salinity stress. Adaptation mechanisms include biochemical pathways that exclude ions or actively transport ions to vacuolar storage areas, and physical adaptations such as cell wall modification or altering the membrane structure [29]. These adaptations can alter membrane permeability in specialized tissues such as roots. Previous studies have documented the salinity tolerance of *E. densa* and *M. simulans* up to 8 g/L [30–31]. *Azolla caroliniana* is not a saline-tolerant species. Studies documented a decrease in *A. caroliniana* biomass and growth when salinity levels increased above 0.05 g/L [32]. The adventitious root structures of *E. densa* emerge from stem nodes and may influence its salinity tolerance [33]. Indeed, *E. densa's* roots are less efficient at transporting ions and acquiring nutrients in general compared with other aquatic macrophytes [19]. The adaptation mechanisms that *M. simulans* and *E. densa* use for survival in saline environments may include enhanced exclusion mechanisms, which may account for the limited AuNP uptake noted in our study. In contrast, *A. caroliniana* is not saline tolerant and exhibited increased absorption of AuNPs into tissues, regardless of NP size. This further supports our hypothesis that plant salinity tolerance may influence AuNP uptake and partitioning.

AuNP sorption rate of the three aquatic macrophytes

When comparing the 18-nm AuNP sorption rate among the three species, *M. simulans, E. densa*, and *A. caroliniana*, we detected no significant difference in the slopes or sorption rates of each treatment over the 24-h exposure (Fig. 6). However, when comparing the 4-nm AuNP sorption rate among *A. caroliniana* and *M. simulans*, the slope was significantly different from that of *E. densa*. These data indicate that absorption of the 4-nm AuNPs is likely for these two species. This is supported further by tissue concentration and electron micrographs. Although the rate of AuNP sorption among the three species does not differ in the 18-nm AuNP treatment, the initial

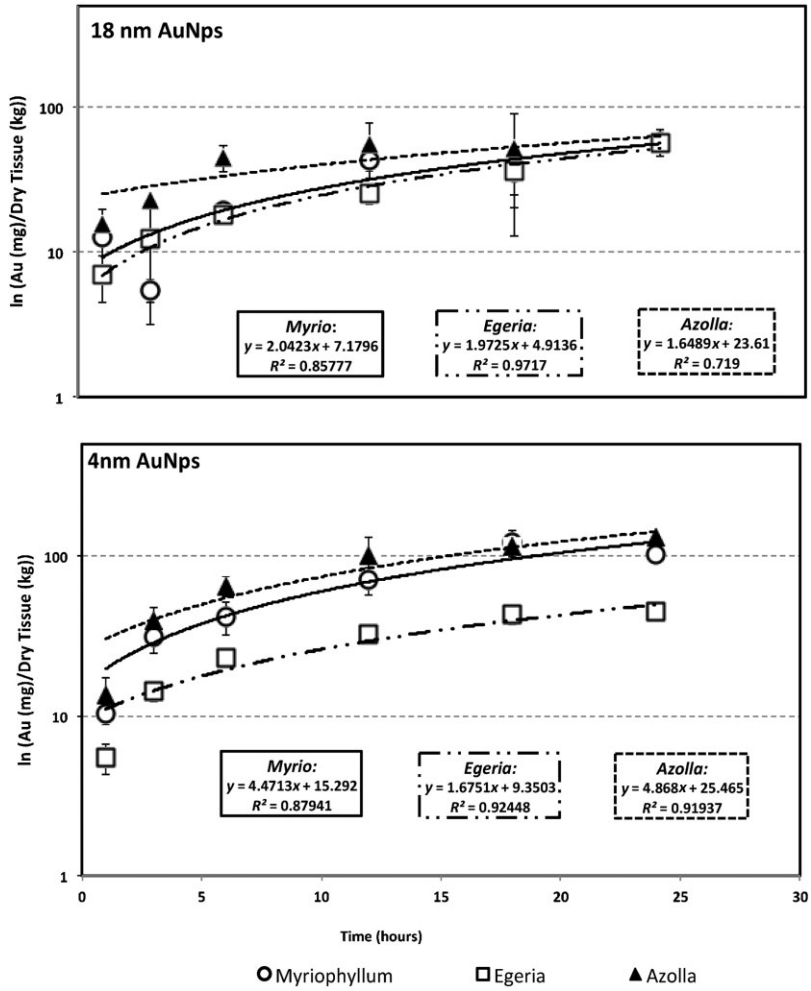

Fig. 6. Comparison of slopes of the sorption rates of Au nanoparticles for *Myriophyllum simulans, Egeria densa*, and *Azolla caroliniana* during 24 h of exposure to 4- and 18-nm Au nanoparticles. Error bars represent standard deviation of the mean.

concentration sorbed with each plant at the 1-h time point differed significantly among species. We attribute this difference in initial sorption to the difference in surface area among the macrophytes. Each of these macrophytes was chosen because of their distinctive leaf morphologies. *Myriophyllum simulans* has finely dissected, needle-like leaves; *E. densa* has whorls of leaves; and *A. caroliniana* has small, compact leaves that fold over one another multiple times. The colorimetric assay revealed that *A. caroliniana* ($35.7 \pm 1.8\,cm^2$) had the highest surface area to mass ratio compared to the other two species. *Myriophyllum simulans* and *E. densa* were very similar in surface area (31.1 ± 0.27 and $31.1 \pm 0.51\,cm^2$; respectively). *Azolla caroliniana* also had the highest initial concentration of Au measured for both 4- and 18-nm AuNPs.

Environmental relevance

Upon harvest, experimental plants were not rinsed but rather were allowed to drip and then were patted dry, to avoid removing loosely adsorbed AuNPs. In the present study, we wished to quantify both adsorbed and absorbed AuNPs. If trophic transfer of nanomaterial can occur in the environment, it does not matter whether NPs are within the tissue or on the surface; however, tissue concentration is important in determining the sorption rates and factors that influence particle sorption. Nanoparticle surface chemistry may also play a vital role in the bioavailability of NPs. Citrate is an organic acid, and many plants exude organic acids (typically malate or citrate) into the rhizosphere and thus alter the surrounding environment to increase nutrient availability or to decrease metal availability in the case of aluminum [34,35]. Because plants normally export organic acids, it is possible that the citrate coatings on the NPs are hindering uptake. These variables should be considered in future uptake studies using nanomaterials with organic surface chemistries.

CONCLUSIONS

This study investigated the potential of 4- and 18-nm citrate-capped AuNPs to sorb with plant tissue. No visual toxicity symptoms to macrophyte tissue were evident over the 24 h of exposure. Both NP sizes adsorbed to all three macrophytes. However, results suggest that 4-nm AuNPs were absorbed by *A. caroliniana* and *M. simulans*. Transmission electron microscopy, SEM, and STEM micrographs support this conclusion. Differences in adsorption and absorption of AuNPs likely are due to the difference in particle sizes and differences among the three plant species. These differences include salinity tolerances and surface area. These results suggest that plant uptake could be an important factor when considering NP fate in aquatic ecosystems and the potential

ability for trophic transfer. Furthermore, bioassays that have longer exposures to AuNPs may provide insight into transport within the plant and potential sequestration.

SUPPLEMENTAL DATA

Figs. S1–S5. (6 MB DOC).

Acknowledgement—We appreciate the assistance of C. Murphy from the University of Illinois at Urbana—Champaign for supplying the 4- and 18-nm AuNPs, J. Hudson and D. Mulwee at Clemson University's Advanced Materials Research Laboratory for electron microscope use, and T. Bruce at Clemson University's Jordan Hall Imaging Facility for Light Microscopy. This research received financial support from grants R833886 and R834092 from the U.S. Environmental Protection Agency's Science to Achieve Results program. J.B. Glenn, S. White, and S. Klaine all contributed to the experiments; J.B. Glenn preformed the experiments and wrote the manuscript. This is Technical Contribution No. 5991 of the Clemson University Experiment Station.

REFERENCES

1. Murphy CJ, Sau TK, Gole AM, Orendorff CJ, Gao J, Gou L, Hunyadi SE, Li T. 2005. Anisotropic metal nanoparticles: Synthesis, assembly, and optical applications. *J Phys Chem B* 109:13857–13870.
2. Sau TK, Murphy CJ. 2004. Room temperature, high-yield synthesis of multiple shapes of gold nanoparticles in aqueous solution. *J Am Chem Soc* 126:8648–8649.
3. Murphy CJ, Gole AM, Hunyadi SE, Stone JW, Sisco PN, Alkilany A, Kinard BE, Hankins P. 2008. Chemical sensing and imaging with metallic nanorods. *Chem Commun* 544–557.
4. Murphy CJ, Gole AM, Stone JW, Sisco PN, Alkilany AM, Goldsmith EC, Baxter SC. 2008. Gold nanoparticles in biology: Beyond toxicity to cellular imaging. *Acc Chem Res* 41:1721–1730.
5. Kelly KL, Coronado E, Zhao LL, Schatz GC. 2003. The optical properties of metal nanoparticles: The influence of size, shape, and dielectric environment. *J Phys Chem B* 107:668–677.
6. El-Sayed MA. 2001. Some interesting properties of metals confined in time and nanometer space of different shapes. *Acc Chem Res* 34:257–264.
7. Colvin VL. 2003. The potential environmental impact of engineered nanomaterials. *Nat Biotechnol* 23:1166–1170.
8. Shukla R, Bansal V, Chaudhary M, Basu A, Bhonde RR, Sastry M. 2005. Biocompatibility of gold nanoparticles and their endocytotic fate inside the cellular compartment: A microscopic overview. *Langmuir* 21:10644–10654.
9. Wigginton NS, Haus KL, Hochella MF. 2007. Aquatic environmental nanoparticles. *J Environ Monit* 9:1306–1316.
10. Limbach LK, Bereiter R, Muller E, Krebs R, Galli R, Stark WJ. 2008. Removal of oxide nanoparticles in a model wastewater treatment plant: Influence of agglomeration and surfactants on clearing efficiency. *Environ Sci Technol* 42:5828–5833.
11. Kiser MA, Westerhoff P, Benn T, Wang Y, Perez-Rivera J, Hristovski K. 2009. Titanium nanomaterial removal and release from wastewater treatment plants. *Environ Sci Technol* 43:6757–6763.
12. Singh RP, Agrawal M. 2008. Potential benefits and risks of land application of sewage sludge. *Waste Manag* 28:347–358.
13. Lin S, Reppert J, Hu Q, Hudson JS, Reid ML, Ratnikova TA, Rao AM, Luo H, Ke PC. 2009. Uptake, translocation, and transmission of carbon nanomaterials in rice plants. *Small* 10:1128–1132.
14. Lee WM, An YJ, Yoon H, Kweon HS. 2008. Toxicity and bioavailability of copper nanoparticles to the terrestrial plants mung bean (*Phaseolus radiatus*) and wheat (*Triticum aestivum*): Plant agar test for water-insoluble nanoparticles. *Environ Toxicol Chem* 27:1915–1921.
15. Lee CW, Mahendra S, Zodrow K, Li D, Tsai YC, Braam J, Alvarez PJJ. 2010. Developmental phytotoxicity of metal oxide nanoparticles to *Arabidopsis thaliana*. *Environ Toxicol Chem* 29:669–675.
16. Ma X, Geiser-Lee J, Deng Y, Kolmakov A. 2010. Interactions between engineered nanoparticles (ENPs) and plants: Phytotoxicity, uptake and accumulation. *Sci Total Environ* 408:3053–3061.
17. Ferry JL, Craig P, Hexel C, Sisco P, Frey R, Pennington PL, Fulton MH, Scott IG, Decho AW, Kashiwada S, Murphy CJ, Shaw TJ. 2009. Transfer of gold nanoparticles from the water column to the estuarine food web. *Nat Nanotechnol* 4:441–444.
18. Maricle BR, Koteyeva NK, Voznesenskaya EV, Thomasson JR, Edwards GE. 2009. Diversity in leaf anatomy, and stomatal distribution and conductance,between salt marsh and freshwater species in the C_4 genus *Spartina* (Poaceae). *New Phytol* 184:216–233.
19. Bristow JM, Whitcombe M. 1971. The role of roots in the nutrition of aquatic vascular plants. *Am J Bot* 58:8–13.
20. Denny P. 1972. Sites of nutrient absorption in aquatic macrophytes. *J Ecol* 60:819–829.
21. Anderson C, Moreno F, Geurts F, Wreesmann C, Ghomshei M, Meech J. 2005. A comparative analysis of gold-rich plant material using various analytical methods. *Microchem J* 81:81–85.
22. Cattaneo A, Carignan R. 1983. A colorimetric method for measuring the surface area of aquatic plants. *Aquat Bot* 17:291–294.
23. Carpita NC. 1982. Limiting diameters of pores and the surface structure of plant cell walls. *Science* 218:813–814.
24. Eichert T, Kurtz A, Steiner U, Goldbach HE. 2008. Size exclusion limits and lateral heterogeneity of the stomatal foliar uptake pathway for aqueous solutes and water-suspended nanoparticles. *Physiol Plant* 134:151–160.
25. Keeley JE. 1990. Photosynthetic pathways in freshwater aquatic plants. *Tree* 5:329–333.
26. Busby CH, Gunning BES. 1984. Microtubules and morphogenesis in stomata of the water fern *Azolla*: An unusual mode of guard cell and pore development. *Protoplasma* 122:108–119.
27. Lin D, Xing B. 2008. Root uptake and phytotoxicity of ZnO nanoparticles. *Environ Sci Technol* 42:5580–5585.
28. Battke F, Leopold K, Maier M, Schmidhalter U, Schuster M. 2007. Palladium exposure of barley: Uptake and effects. *Plant Biol* 10:272–276.
29. Parida AK, Das AB. 2004. Salt tolerance and salinity effects on plants: A review. *Ecotoxicol Environ Saf* 60:324–349.
30. Hauenstein E, Ramirez C. 1986. The influence of salinity on the distribution of *Egeria densa* in the Valdivia river basin, Chile. *Arch Hyrobiol* 107:511–519.
31. Goodman AM, Ganf GG, Dandy GC, Maier HR, Gibbs MS. 2010. The response of freshwater plants to salinity pulses. *Aquat Bot* 93:59–67.
32. Haller WT, Sutton DL, Barlow WC. 1974. Effects of salinity on growth of several aquatic macrophytes. *Ecology* 55:891–894.
33. Sorrell BK, Dromgoole FI. 1987. Oxygen transport in the submerged freshwater macrophyte *Egeria densa* planch. I. Oxygen production, storage and release. *Aquat Bot* 28:63–80.
34. Ligaba A, Shen H, Shibata K, Yamamoto Y, Tanakamaru S, Matsumoto H. 2004. The role of phosphorus in aluminum-induced citrate and malate exudation from rape (*Brassica napus*). *Physiol Plant* 120:575–584.
35. Lipton DS, Blanchar RW, Blevins DG. 1987. Citrate, malate, and succinate concentrations in exudates from P-sufficient and P-stressed *Medicago sativa* L. seedlings. *Plant Physiol* 85:315–317.